Pseudomonas aeruginosa PA5oct jumbo phage reduces planktonic and biofilm population and impacts its host virulence through a pseudolysogeny event

Tomasz Olszak[1], Katarzyna Danis-Wlodarczyk [1,2,#], Michal Arabski[3], Grzegorz Gula[1], Slawomir Wasik[4], Gerard Higgins [5,6], Brian J. Harvey[6], Rob Lavigne[2], Zuzanna Drulis-Kawa[1]*

[1]Department of Pathogen Biology and Immunology, Institute of Genetics and Microbiology, University of Wroclaw, Wroclaw, Poland

[2]Laboratory of Gene Technology, KU Leuven, Leuven, Belgium

[3]Department of Biochemistry and Genetics, Institute of Biology, The Jan Kochanowski University in Kielce, Kielce, Poland

[4]Department of Molecular Physics, Institute of Physics, The Jan Kochanowski University in Kielce, Kielce, Poland

[5]National Children Research Centre, Dublin, Ireland

[6]Department of Molecular Medicine, Royal College of Surgeons in Ireland, Education and Research Centre, Beaumont Hospital, Dublin, Ireland

current affiliation: Department of Microbiology, Ohio State University, Columbus, OH, United States

*Corresponding author.

E-mail: zuzanna.drulis-kawa@uwr.edu.pl (ZDK)

Abstract

In this work we assess critical parameters to assess the *in vitro* capacity of the novel "jumbo" phage PA5oct for phage therapy by studying its impact on the planktonic and biofilm population of *P. aeruginosa*. PA5oct is the third largest (in terms of the genome size) *Pseudomonas* phage with a specific spectrum of lytic activity (infects 24% of strains from the international *P. aeruginosa* reference panel and 68% of clinical strains from the Belgian Military Hospital Neder-Over-Heembeek). *In vitro* studies using the airway surface liquid (ASL) model demonstrate that PA5oct effectively inhibits the growth of planktonic population of *P. aeruginosa*. Interferometric measurements of a 72-hour biofilm also prove the contribution of PA5oct in biofilm matrix degradation. Biofilm-derived PA5oct phage-resistant mutants often show cross-resistance to both LPS-dependent and only closely related fimbriae-dependent phages. This phage resistance is mostly associated with PA5oct phage pseudolysogeny event which strongly reduces bacterial *in vivo* virulence. These properties can be considered as key assets in using this bacterial virus in phage therapy settings.

Importance

An important aspect of phage therapy is the efficacy of bacterial eradication and emergence of phage-resistant mutants. Here we present the consequences of PA5oct jumbo phage treatment of planktonic and sessile *P. aeruginosa* cells. Apart of efficient bacteria eradication and biofilm degradation, PA5oct introduces stable pseudolysogeny in most of phage-resistant clones. Moreover, phage episome is related to reduced bacterial virulence and clearance by innate immune system of infected host. This is in contrast to the current knowledge about pseudolysogeny as an temporary stage in dormant cells, mostly having no influence on bacteria. In treatment, the pseudolysogeny is considered as an adverse effect giving phage-resistance, but our results prove that this event may lead to diminished bacterial virulence and clearance from infected host. The above findings provide new insights into general knowledge of the host-parasite interactions between lytic phages and bacteria and can impact the application of phage therapy in general.

Keywords: giant bacteriophage, *Pseudomonas aeruginosa*, biofilm, Airway Surface Liquid Infection model, phage-resistant mutants, pseudolysogeny

Introduction

Finding a solution to the antibiotic resistance problem is one of the greatest challenges of modern science and medicine, and the search for alternative methods of antibacterial therapy has led to the reappraisal of bacteriophages (1). Phage therapy efficacy studies (2–4) and recent advances in the regulatory frame, in which phage therapy can be adopted as part of 'Magistral preparations' (5) have shifted the focus from proving efficiency to its implementation and the expansion of available phage for phage therapy cocktail design.

Among phages being evaluated for phage therapy applications, are the jumbo phages, which contain dsDNA genomes in excess of 200kb (6). Generally, Jumbo phages can be found in various historical commercial phage therapy products, as they have a broad host range. This is explained by the large coding potential of jumbo phage, allowing them to be (partly) independent from the bacterial enzymes (7). However, some are marked with a high frequency of transduction, impacting the evolution of bacteria and raising questions on the safety of use of this phages in therapy (8). Although the first "jumbo phage" has been discovered over 40 years ago (*Bacillus* bacteriophage G), the frequency of giant phages isolation remains rather low (less than 90 complete genomes in GenBank database), but is surging in recent years. This group is incredibly diverse, since newly isolated jumbo phages generally show low similarity to those present in public databases. Furthermore, annotated genomes contain a vast majority of genes with undefined function (9).

The first fully sequenced „jumbo phage" specific for *Pseudomonas aeruginosa* was the phiKZ - a giant lytic myovirus with a broad host range, isolated in Kazakhstan. Its large capsid (120 nm in diameter) encloses a linear, circularly permuted, terminally redundant genome (280,334 bp, 36.8% G+C) and is capable of carrying large fragments of the bacterial DNA (generalized transduction) (10). This phage has become a hallmark example for structural analysis of phage particle and for genetic and structural analysis (11–13). Currently, over twenty giant *Pseudomonas* bacteriophages within the diverse phiKZ-like clade have been isolated: 31, Lin21, Lin68, NN, LBG20-23, LBG26, PBD1-4, PTB80, phiST-1, EL, RU, OBP, Lu11, Psp3, Col21, 201phi2-1, phiPA3 and KTN4 (8, 14, 15).

Pseudomonas aeruginosa phage PA5oct was recently isolated from sewage samples in Wroclaw, Poland as a representative of completely new genus of *Myoviridae* family. Analysis of the virion morphology (TEM micrograph) and genome sequencing ranks PA5oct phage among the largest known bacterial viruses. The diameter of PA5oct head is about 131 nm and its tail is about 136 nm long (16). PA5oct has linear A-T rich (33.3% GC) dsDNA genome

containing 287,182 bp (3rd biggest genome of *Pseudomonas* phage and 8th among *Myoviridae* family) and for which a comprehensive temporal transcriptome analysis, structural proteomics analysis and host transcription response has been studied (Danis-Wlodarczyk et al., in submission).

In this study we assess the efficacy of PA5oct giant phage as antimicrobial agent. For this, we apply an integrated approach for the *in vitro* preclinical evaluation of phage therapy in *Pseudomonas* infections using the laser interferometry technique to measure the biofilm eradication dynamics and an advanced Airway Surface Liquid infection model, which mimics *in vitro* the normal and CF lung environments.

Results

The host range of phage PA5oct suggests an increased activity against clinical isolates

Lytic phage PA5oct has been isolated from sewage sample collected from irrigated fields and is classified to the Order *Caudovirales*, Family *Myoviridae*, as a giant phage (16). The PA5oct genome, transcriptome and proteome has been presented elsewhere (Danis-Wlodarczyk et al., in submission). The lytic activity (host range) of PA5oct was examined on two independent *P. aeruginosa* panels. First, 43 clinical *P. aeruginosa* strains from COST international reference panel were used (17). For this collection phage PA5oct infects 24% isolates, which is more limited compared to representatives of *Luz7virus* LUZ7 (42%), *Phikmvvirus* group (LUZ19 44%), *Pbunavirus* group (LBL3 40%, KT28 28%, KTN6 42%) and *Phikzvirus* group (phiKZ 47%, KTN4 33%). For a second collection of 57 clinical strains from Military Hospital Neder-Over-Heembeek, Brussels, Belgium collection (18) marked differences can be observed when compared to *Pseudomonas* broad set of phage, including the *Luz7virus* LUZ7, *Lit1virus* LIT1, *Luz24virus* LUZ24, *Phikmvvirus* group (LUZ19, LKD16, LKA1, KMV), *Pbunavirus* group (LBL3, LMA2, LSL4, KT28, KTN6) and the giants (phiKZ KTN4) (Table S1-S2). PA5oct infects 68% strains, whereas LUZ7 32%, LIT1 12%, LUZ24 19%, *Phikmvvirus* group (LUZ19: 37%, LKD16: 32%, LKA1: 4%, KMV: 33%), *Pbunavirus* group (LBL3: 46%, LMA2: 25%, LSL4: 18%, KT28: 60%, KTN6: 68%) and giants *Phikzvirus* (phiKZ 63%, KTN4 46%). Although, the international reference panel also contains 25 isolates causing the infection in cystic fibrosis patient (CF) and PA5oct phage lyses six of them, no correlation can be observed in terms of phage activity versus CF early/late type of *P. aeruginosa* isolate. In general, the above results indicate an antibacterial potential of PA5oct against clinical *P. aeruginosa* strains isolated from different kind of infections (burn, CF-patients pneumonia, nosocomial pneumonia, urinary tract infection).

Propagation experiments on a panel of defined knock-out PAO1 mutants of the cell wall reveal that PA5oct requires the presence of LPS and at least a second host cell surface receptor, like the Type IV pili (Table 1). The flagella mutant ΔfliC wt algC wt pilA did not provide conclusive results concerning the susceptibility to phage infection.

Table 1. Phage receptor identification on *P. aeruginosa* PAO1 mutants.

PAO1 isolates	**Phenotype**	**PA5oct activity**
ATCC 15692	Wild type	+
PAO1 strain Pirnay*	Wild type with inactive Type IV pili	-/+
PAO1 strain Krylov*	Wild type	+
Δrmd (A-, B+)**	Deficiency in D-rhamnose biosynthesis; lack of A-band LPS	+
ΔwaaL (A-, B-)**	Lack of WaaL ligating O-polymer to core-lipid A; LPS is devoid of A-band and B-band, semirough (SR-LPS, or core-plus-one O-antigen)	-/+
ΔwbpL (A-, B-)**	Lack of glucosyltransferase WbpL essential for initiation of both A-band and B-band synthesis	-
ΔfliC ΔalgC ΔpilA***	Lack of flagella; lack of AlgC required for A-band, core oligosaccharide, and alginate biosynthesis; lack of Type IV pili	-
ΔfliC wt algC ΔpilA***	Lack of flagella; lack of Type IV pili	-
ΔfliC wt algC wt pilA***	Lack of flagella	-/+
wt fliC wt algC wt pilA***	Wild type	+

* Military Hospital Neder-Over-Heembeek, Brussels, Belgium, Dr. Jean-Paul Pirnay
**Laboratory of Foodborne Zoonoses, Guelph, Canada, Andrew M. Kropinski
***Technical University Hamburg, Germany, Max Schöbert

Phage PA5oct efficiently reduces planktonic P. aeruginosa in an Airway Surface Liquid infection model

The *in vitro* antibacterial activity of PA5oct against planktonic bacteria is assessed using the ASL model on normal NuLi-1 and cystic fibrosis CuFi-1 bronchial epithelium cell lines (15, 19) to mimic a natural environment of *Pseudomonas* lung infection both in healthy and cystic fibrosis patients. Three different, well-characterized *P. aeruginosa* strains have been applied, including a standard PAO1, burn-infection strain nonCF0038 and small colony variant CF708, isolated from the late stage of CF infection (20). Moreover, the epithelial cells viability controls were established as well, and no toxicity influence was observed for phage and bacterial samples for particular experimental parameters.

After infection of both epithelial cell lines for 3 h, the colony count shows that all *P. aeruginosa* strains efficiently propagate in both ASLs (10^7 - 10^9 cfu/ml). Phage treatment significantly ($p <$

0.05) reduces the CFU counts for normal NuLi-1, where a 4.5 log, 6.5 log and 3 log decrease is observed for PAO1, nonCF0038 and CF708, respectively (Fig. 1A). The phage application for CuFi-1 epithelia infection is also very effective ($p < 0.05$) giving 5 log, 2.5 log and 5 log reductions in CFU of PAO1, nonCF0038 and CF708, respectively (Fig. 1B).

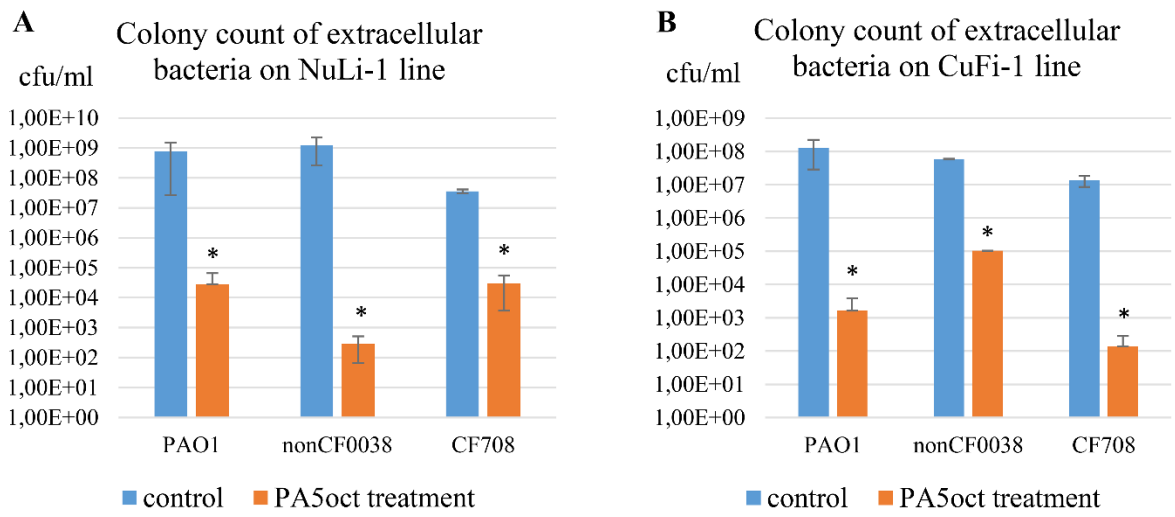

Figure 1. Phage PA5oct treatment of *P. aeruginosa* infecting NuLi-1 (A) and CuFi-1 epithelial cells (B). Colony count of bacteria collected from apical wash. The orange bars represent bacteria titers after 1.5 h of incubation with PA5oct phage. The blue bars represent controls without phage treatment. The error bars indicate the standard deviation. The results are presented as the means ± SD. Statistical analysis was made by the ANOVA test (denoted *p*-values < 0.05). (*) *p*-values < 0.05.

Antibacterial efficacy of PA5oct phage against biofilm-living PAO1

When using laser interferometry to study biofilm formation, a hydrophilic Nephrophane membrane (scaffold) is overgrown by a 72 h PAO1 biofilm. The diffusion of TSB medium through the biofilm layer is then evaluated, which correlates with the structural degradation of the biofilm, after treatment with active and UV-inactivated PA5oct phage. The diffusion rate of medium transported through the intact biofilm-covered membrane after 40 min (0.605 mg) is significantly lower than for biofilm ($p < 0.05$) after active and inactivated phage treatment, reaching 1.64 mg and 1.17 mg, respectively (Fig. 2). The increase of the diffusion obtained after the application of inactivated particles may be explained by virion-associated proteins responsible for biofilm matrix degradation.

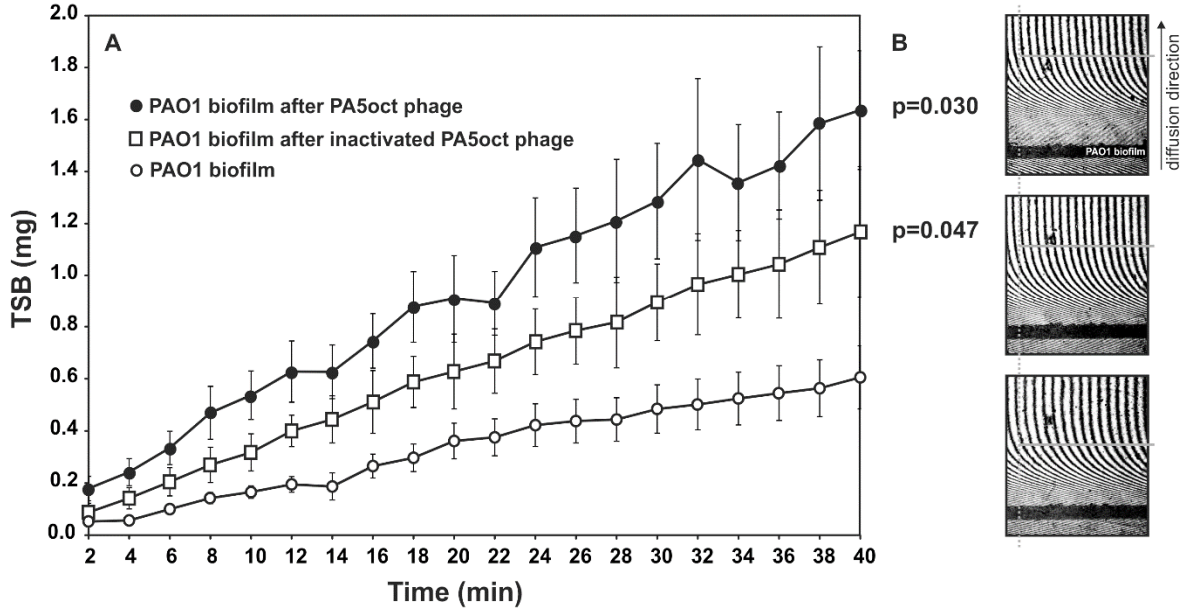

Figure 2. Laser interferometry analysis of TSB medium diffusion through PAO1 biofilm treated with PA5oct phage. Untreated biofilm was used as control. Error bars denote SD. The results displayed are the mean of three independent experiments. Statistical analysis was made by the ANOVA test (A). The examples of interferograms (40 min) for PAO1 biofilm treated with active and inactivated PA5oct phages as well as control (from the top of the panel) (B).

To further establish the antimicrobial activity of PA5oct phage against biofilm-living bacteria, complementary assays have been performed: biomass CV staining and the measurement of pyocyanin and pyoverdin/pyochelin secretion (Fig. 3). Experiments were performed on the PAO1 biofilm grown on a Nephrophane membrane for three time periods (24, 48 and 72 h). The CV staining of biofilm biomass eradication shows a significant effect of active PA5oct against 72 h-old biofilm after 4 h treatment. Moreover, the analysis of pyocyanin and pyoverdin/pyochelin secretion indicate that active phages significantly decrease the level of this compound for the tested biofilms (72 h) and that UV-inactivated phages have no significant effect. A positive correlation between biofilm formation, pyocyanin and pyoverdin/pyochelin levels has been found in the supernatants, indicating that the reduced levels of *Pseudomonas*-specific compounds are correlated to the phage activity. In general, it can be concluded that phage PA5oct primarily affects maturate biofilms reducing its biomass as well as some virulence factors.

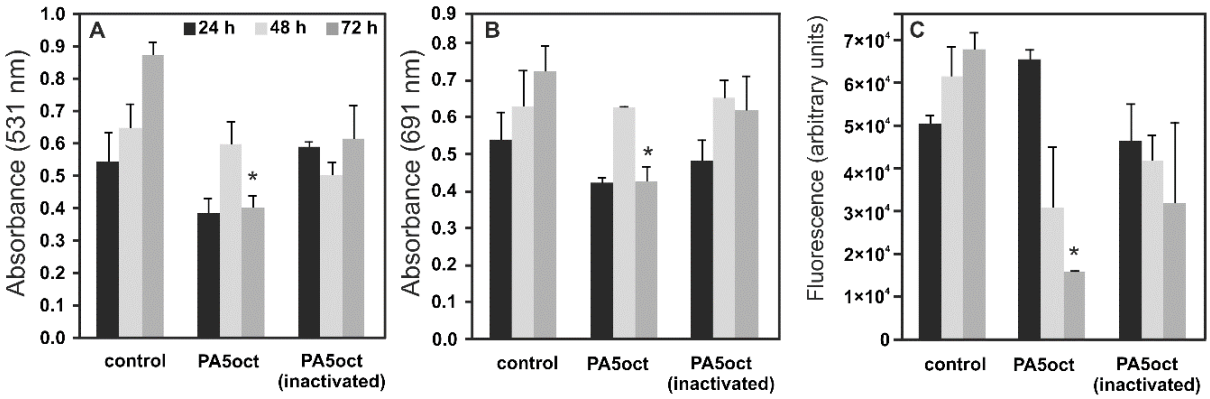

Figure 3. The anti-biofilm effect of PA5oct phage treatment (4 h) on 24, 48 and 72 h PAO1 biofilm formed on Nephrophane membrane. The biomass evaluation by CV staining (A); the level of pyocyanin in growth medium (B); the fluorescence of pyoverdin in growth medium (C). Untreated biofilm was used as control. The results are presented as the means ± SD. Statistical analysis was made by the ANOVA test (denoted p-values < 0.05).

Phage PA5oct impact on PAO1 biofilm-living population after treatment

An important aspect of this study is the evaluation of the impact of PA5oct phage introduction to the biofilm population. For this purpose thirty randomly taken colonies were selected from 24, 48 and 72-hours biofilm after phage treatment and checked for phage susceptibility. At the same time, thirty control clones from untreated biofilm were isolated. About one third of suspected mutants and a 100% of control isolates still remain susceptible to PA5oct infection, whereas 20 clones become resistant. In the next step, isolates are examined for cross resistance to other phages lytic to PAO1 wild type strain (Table S1), recognizing different receptors: Type IV pili-dependent (phiKZ, KTN4, LUZ19), LPS-dependent (KT28, KTN6, LUZ7) and phage with an unverified receptor (LBL3). Control isolates and PA5oct-sensitive clones taken from the biofilm after phage treatment retain the same phage typing pattern as PAO1 wild type. In general, we can distinguish five different phage typing patterns (Table 2).

Table 2. Phage typing of PA5oct clones obtained during biofilm treatment

Bacterial clones	sensitivity to phage infection							
	LPS/pili		LPS-dependent			pili-dependent		
	PA5oct	LBL3	KT28	KTN6	LUZ7	KTN4	phiKZ	LUZ19
control planktonic PAO1	+	+	+	+	+	+	+	+
control biofilm PAO1	+	+	+	+	+	+	+	+
PA5oct resistant type 1	-	-	+	+	+	-	+	+
PA5oct resistant type 2	-	-	+	+	+	-	-	+
PA5oct resistant type 3	-	+	-	-	+	-	+	+
PA5oct resistant type 4	-	+	-	-	+	+	+	+
PA5oct resistant type 5	-	-	-	-	+	+	+	+

(+) sensitive to phage infection; (-) resistant to phage infection;

In most cases, cross-resistance patterns match to *Pbunavirus* phages (*Myoviridae*), recognizing mostly LPS structure. However, some PA5oct-resistant clones are resistant to LBL3 phage (*Pbunavirus*) and Type IV pili-dependent giant phages (phiKZ and KTN4). Interestingly, these strains are still susceptible to phages KT28 and KTN6. Three mutants exhibiting resistance to KTN4 phage remain susceptible to phiKZ, very closely related to the latter one (> 99% genome-wide DNA homology) (15). This results implies the requirement for PA5oct of two different receptors for effective infection. Interestingly, no cross-resistance is observed for podoviruses (LUZ7 and LUZ19), despite their dependence on the same bacterial surface macromolecules for infection.

Emerging phage PA5oct resistant mutants show a reduced virulence

To evaluate the correction between phage receptor modification in emerging phage-resistant population and the principal virulence factors of these mutant strains, we evaluated LPS composition, motility parameters, biofilm formation, pro-inflammatory response in monocytes and *in vivo* virulence properties using a *Galleria* model. (Table 3, Fig. S1-S3).

For these analyses, it is important to note that all selected phage-resistant mutants exhibit the same growth rate/size of colonies as the parental PAO1 controls. The analysis of LPS extracted from PA5oct phage-resistant mutants, shows a dramatic O-antigen truncation in the majority of 7/10 of tested mutants (Fig. S1), while the remaining strains presumably have indiscernible changes, since another LPS-dependent phage (LBL3) shows cross-resistance. For these mutants, the flagellum-dependent swarming motility increased in five out of ten of the PA5oct phage-resistant isolates. Interestingly, intensification of flagellum-associated movement was

almost exclusively associated to strains with truncated LPS O-chain. In nine out of ten of the tested isolates the ability of fimbriae-related and swimming movement were unaffected. Biofilm formation varies greatly, without correlation to other tested biological features. Based on the mutants PA5oct phage infection probably does not affect the production of the redox-active phenazine nor siderophores, since PA5oct phage-resistant mutants showed a comparable pyoverdine and pyocyanin production (Table 3).

Table 3. The virulence features of PA5oct resistant clones.

Type of isolate	Name	LPS	Biofilm		Swimming motility		Swarming motility		Twitching motility		Pyocyanin		Pyoverdine		THP1-Xblue stimulation	*Galleria* survival after 48h [%]	PCR
			[OD_{590}]	SD	growth zone [mm]	SD	growth zone [mm]	SD	growth zone [mm]	SD	[OD_{695}]	SD	[RFU]	SD			
Control biofilm	PAO1/B	S	0.7	0.1	16.9	3.6	6.3	1.1	18.2	1.1	0.2	0.0	2878.7	49.5	-	0/0	-
Control planktonic	PAO1	S	0.8	0.1	22.8	4.2	7.2	0.4	24.2	1.2	0.2	0.0	3190.9	16.9	-	0/0	-
PA5oct resistant type 1	48/F	S	0.6	0.1	14.0	3.0	7.3	1.2	17.0	1.1	0.2	0.0	2921.1	28.4	-	10	-
PA5oct resistant type 2	48/A	S	0.9	0.1	22.0	3.7	7.7	2.9	17.7	1.5	0.1	0.0	3482.9	31.0	+	80	+
PA5oct resistant type 2	48/H	S	0.3	0.1	9.3	1.9	4.8	1.8	8.8	0.8	0.8	0.1	2875.5	12.3	+	80	+
PA5oct resistant type 3	24/D	R	0.9	0.1	24.0	4.6	8.2	0.4	21.0	1.3	0.1	0.0	2838.4	29.8	+	90	+
PA5oct resistant type 3	48/E	R	0.3	0.1	19.8	2.3	6.5	1.4	10.0	1.7	0.1	0.0	3068.7	26.9	+	50	+
PA5oct resistant type 4	48/I	R	1.0	0.1	23.2	0.4	5.7	0.5	13.8	0.4	0.1	0.0	3043.2	15.3	+	50	+
PA5oct resistant type 4	72/I	R	0.3	0.1	23.3	2.4	9.2	1.5	15.3	3.2	0.1	0.0	2961.7	63.7	+	80	+
PA5oct resistant type 5	24/G	R	0.8	0.1	21.0	3.0	8.3	0.8	19.3	1.0	0.1	0.0	2845.7	10.3	+	50	+
PA5oct resistant type 5	72/A	R	1.3	0.2	16.3	1.0	8.2	0.4	22.2	1.5	0.2	0.0	1574.1	60.2	+	90	+
PA5oct resistant type 5	72/D	R	1.6	0.2	22.2	3.9	10.3	0.5	20.8	0.8	0.1	0.0	2790.9	38.3	+	80	+

S- smooth LPS; R- rough LPS

These microbiological properties already hint towards an impact on virulence, which could prove to be a key advantage for the use of this phage in phage therapy settings. To validate this further, we examined the virulence features characteristics by *in vivo* infection in *G. mellonella* larvae, assessing their survival as a function of time (Fig. S2). Using equal doses of bacteria (10 µl of 10^3 cfu/ml) nine out of ten phage-resistant mutants show a dramatically diminished virulence ($P < 0.05$). The larvae survival rate at 48 h and 72 h post infection varies from 50-90% and 40-90%, respectively, in comparison to 0% after 48 h for control biofilm PAO1 infection and one mutant (48F). In parallel, we determined the TLR stimulation profile of THP1-XBlue™ cell line when treated with PA5oct-resistant culture filtrates. The TLRs serve as Pattern Recognition Receptors (PRRs) playing a crucial rule in the proper functioning of the innate immune system. Fully consistent with our *in vivo* data, the same mutants gained pro-inflammatory features, strongly stimulating monocyte culture comparing to controls PAO1 parental isolate (Table 3, Fig. S3).

The reduced virulence in the phage resistant mutants is associated with a pseudolysogeny event

To further characterize the molecular basis for this reduced virulence, PFGE analysis revealed an unexpected result. In nine out of ten of tested isolates PFGE analysis of total bacterial DNA confirmed the presence of phage DNA as an episome, present as a separate band around 300-400 kbp, consistent with the PA5oct genome size. (Table 3, Fig S4-S5). A PCR assay targeting the gene encoding the major head subunit precursor confirmed this observation. Indeed, only the mutant that showed the same pro-inflammatory activity and *in vivo* virulence as the wild type and control biofilm PAO1 strains was free of phage DNA. This observation warrants additional research.

Discussion

The principal aim of this study was to assess the suitability of *Pseudomonas* virus PA5oct for phage therapy applications, using our suite of preclinical evaluation methods.

The ASL experiments confirm PA5oct can efficiently access and infect planktonic cells in mucous conditions, but remain dependent on the strain used, as previously observed for giant *Pseudomonas* KTN4 phage (15, 21). According to a study by Worlitzsch *et al.* (21), *P. aeruginosa* does not interact the CF epithelium directly, but rather gets stuck in mucus plugs formed in the airways. From this perspective, it is a major advantage that phage PA5oct diffuses through dense mucus without major problems and is most active on mature 72-hour biofilms, as indicated by our two complementary assays (permeability assay and Nephrophane membrane

biofilm assay). This observation contradicts the general belief that phages have the greatest activity against immature biofilms, composed of metabolically active cells (22, 23). In the case of PA5oct, biofilm biomass reduction occurs only as a result of phage-mediated cell lysis, whereas biofilm matrix may be degraded by both active and inactivated phages (noticeable increase of TSA diffusion trough the Nephrophane membrane). This result may suggest that PA5oct phage destroys the biofilm not only by unsealing its structure as a result of lysing tightly packed cells, but it may also express enzymes (polysaccharide depolymerases) which disrupt the biofilm matrix (24).

A key element in the establishment of phage PA5oct as part of a therapeutic cocktail is phage receptor analysis. For giant phage PA5oct, knock-out strains and cross resistance experiments reveal a dependence on LPS as the primary receptor and Type IV pili as the secondary receptor. This versatility can in general explain the broad spectrum of lytic activity of jumbo phages. In our case, the radically different host range between both host range panels is noteworthy. In the reference panel of *P. aeruginosa* (BCCM / LMG), containing 25 out of 43 strains isolated from patients with cystic fibrosis (25), only 24% of the strains show susceptibility to PA5oct phage with 6 from CF patients (17), whereas phage PA5oct infects 68% of isolates from our standard clinical strain panel. This is indicative of specific phenotypes associated with isolates from CF patients, including reduced virulence patterns compared to environmental strains, including a modified LPS structure, lower expression of Type IV pili and flagellum and a decrease of production intensity of alginate, pyocyanin, pyoverdine and elastase (26–28).

The introduction of PA5oct phage into the biofilm population of *P. aeruginosa* triggers inevitable formation of mutants resistant to this virus. The PA5oct phage-resistant clones, subjected to typing with a panel of phages recognising different receptors, show that the genetic changes under the influence of PA5oct pressure go far beyond the modulation of a single receptor. PA5oct resistant isolates show cross-resistance to phages from different groups, and the typing patterns are very diverse, suggesting major genomic rearrangements in the bacterial genome which impact multiple receptors (29, 30), which can be studied further.

The formation of phage-resistant bacterial mutants is often considered as a standard criticism and weakness of phage therapy. Although phage-related phenotypic changes in bacteria decrease the efficacy of phage therapy as a standalone therapy, in practice it turns out, that the occurring phenotypic modifications usually lead to a diminished bacterial virulence. As a consequence, the bacterial population that survived the phage therapy becomes sensitive to the immune system that effectively removes the pathogenic agent (4).

A somewhat forgotten phenomenon of pseudolysogeny for many years was regarded as a temporary stage of phage particle dormancy. However, it appears that the presence of episome inside the host cell influences its phenotype and contributes the cross-resistance to other bacteriophages as well (31, 32). The giant phages are known to easily undergo episome formation as was previously reported for phiKZ phage (33). In this study we indicated the presence of a pseudolysogeny event of PA5oct giant phage which strongly affect the virulence of bearing PAO1 population. These pseudolysogens show an increased pro-inflammatory stimulation in monocytic cells enhancing the clearance mechanisms of innate immune system. As the consequence significant survival improvement was seen in infected moth larvae. As the result those mutants became significantly less virulent *in vivo* in comparison to wild-type PAO1 and phage-resistant mutant without PA5oct episome. This effect could potentially be directly or indirectly induced by phage PA5oct genes expressed in pseudolysogeny state. Taking into account that the prevalence of PA5oct pseudolysogenic mutants was relatively high (90% of sessile cells) we may conclude that this specific giant phage PA5oct efficiently eradicates sensitive *P. aeruginosa* cells both planktonic and sessile, while at the same time selects for a primarily non-virulent pseudolysogenic resistant population. Overall, these observations show that PA5oct has an interesting potential as part of a therapeutic cocktail, based on its versatility, its specific activity towards mature biofilms and its targeting of virulence factors as receptor. However, its specificity towards groups of isolates also focuses its applicability and efficiency towards specific cases. This in turn implies the need for the establishment of adaptable phage cocktails, tailored towards verified hosts, rather than fixed cocktails to serve broad applications in a generic sense.

Materials and Methods

Bacteriophages propagation and purification

Phage PA5oct was propagated as previously described by Danis-Wlodarczyk (34). Phage lysate was purified by 0.45 and 0.22 µm filtration and the incubation with 10% polyethylene glycol 8000 (PEG 8000) – 1 M NaCl according to standard procedures (35). Finally, the CsCl-gradient ultracentrifugation was applied (36) and phage preparation was dialyzed 3 times for 30 min against 250 volumes of phage buffer using Slide-A-Lyzer Dialysis Cassettes G2 (Thermo Fisher Scientific Inc, MA, USA). The phage titre was assessed using the double-agar layer technique (37) and purified samples were stored at 4°C in the dark.

Phage host range and phage receptor analysis

The bacterial susceptibility to phage-mediated lysis was determined by spot test technique applying 10^5 pfu/ml phage titer (38). The phage receptor on bacterial surface was tested on PAO1 knock-out mutants deficient in biosynthesis of A-band and B-band O-antigen, flagella, Type IV pili, or alginate production (Table 1). The phage host range was evaluated on 57 clinical strains from Military Hospital Neder-Over-Heembeek, Brussels, Belgium collection (18) and compared to other *Pseudomonas* phages listed in Table S1-S2.

Airway Surface Liquid infection model

For the Airway Surface Liquid (ASL) experiments, two cell lines (NuLi-1; Normal Lung, University of Iowa), isolated from human airway epithelium of normal genotype and CuFi-1; Cystic Fibrosis, University of Iowa, isolated from bronchial epithelium of a CFTR F508del/F508del patient) were used (kindly provided by prof. Zabner, University of Iowa, Iowa City, IA). The ASL model was prepared according to methods described by Zabner (19). The experiment was conducted as previously described (15). In short, cell lines were infected with the *P. aeruginosa* PAO1 reference strain (6.2×10^7 cfu/ml), nonCF0038 isolate from burn wound (6.5×10^7 cfu/ml) and CF708 small colony variant (1.0×10^6 cfu/ml) and incubated for 1.5 h at 37°C, 5% CO_2. Next, a 25 µl volume of the PA5oct phage lysate (6×10^8 pfu/ml) was added to each millicell hanging cell culture insert, which were further incubated for 1.5 h at 37°C, 5% CO_2. To evaluate the phage efficacy in bacteria eradication, cells after treatment were washed with PBS and CFU counts were calculated from apical washes on LB agar (Sigma-Aldrich). The data were analyzed using the Statistica software package (StatSoft, Tulsa, OK, USA). All the values were expressed as mean ± SD and significant differences between variations (denoted p-values < 0.05) were assessed by means of the Snedecor-Fisher test using one-way ANOVA.

Biofilm eradication analysis on Nephrophane membrane

The ability of PA5oct phage to degrade biofilm matrix was evaluated by laser interferometry method (15). PAO1 biofilm was formed for 72 hours at 37°C in Trypticase-Soy broth (TSB, bioMerieux, France), as the level of membrane coverage by biofilm was determined as 92.4%. Next, the biofilm was treated for four hours at 37°C with intact and UV-inactivated phage suspensions (5×10^8 pfu/ml). The degradation of biofilm was assessed as the permeability increase of its matrix for low molecular compounds (TSB). The quantitative measurements of TSB diffusion through biofilm structure treated with phage was tested by laser interferometry method (15, 34). The data was analyzed using the Statistica software package (StatSoft, Tulsa,

OK, USA). All values were expressed as mean ± SD and significant differences between variations (denoted p-values < 0.05) were assessed using the Snedecor-Fisher test using a one-way ANOVA.

Biofilm eradication was also examined by crystal violet (0.004%) staining for 15 min as previously described (15) and tested for pyocyanin and pyoverdin/pyochelin levels in the supernatants as described below.

Isolation of phage resistant mutants from treated biofilm

P. aeruginosa PAO1 mutants resistant to PA5oct phage were isolated by the controlled infection. In the first step, bacterial suspension in TSB was incubated (37°C) in 96-well peg-lid plate (Nunc, Denmark) for 24, 48 or 72 hours enabling bacteria to form biofilm. Afterwards, the mature biofilm molded on the surface of pegs was immersed in phage PA5oct suspension (10^6 pfu/ml) for 24 hours. Finally, pegs were washed with PBS buffer to clear away planktonic bacteria and the biofilm population was collected using an ultrasonic bath, and then plated on TSA (bioMerieux) for 24 h at 37°C, to isolate discrete colonies. Ten randomly taken isolates from each time point, were passaged five times on TSA to confirm the stability of genetic changes. Thirty control non-treated biofilm strains were isolated in an analogous manner. The emerging PA5oct phage-resistant clones were verified by spot technique, applying 10^5 pfu/ml PA5oct phage titer (38). Moreover, the clones were also tested the same way in terms of the susceptibility to other *Pseudomonas* phages: Type IV pili-dependent (phiKZ, KTN4, LUZ19), LPS-dependent (KT28, KTN6, LUZ7) and a phage with an unverified receptor (LBL3) (Table S1). All tests were performed in triplicate.

Pyocyanin and pyoverdine production

The level of pyoverdine and pyocyanine production was analyzed on a 72h-biofilm formed on Nephrophane or selected PAO1 mutants cultured (48 hours, 37°C) in TSB medium (bioMerieux, France) in a 24-well polystyrene plate (Sarstedt, Germany) (34). To investigate the level of pyocyanin production the supernatant absorbance was measured at $\lambda = 695$ nm. For pyoverdine production the fluorescence was measured at $\lambda ex = 392$ nm and $\lambda em = 460$ nm.

Motility assays

Solid surface bacterial movement dependent on Type IV pili, called “twitching motility” was measured by perpendicular stabbing a toothpick through the agar layer (up to the bottom of the plate) and 0.01% crystal violet to visualize the growth zone according to Turnbull &

Whitchurch (39). Flagellum dependent movement in liquid medium (swimming motility) and semi-liquid medium (swarming motility) was evaluated using technical agar (Becton-Dikinson, USA) at either 0.3% (swimming motility) or 0.8% (swarming motility) as described by Ha et al. (40, 41). The swimming and swarming motility assays inoculation was limited to shallow, perpendicular stabbing the outer layer of agar. The growth zone results for twitching and swimming/swarming are presented as the mean of ten replicates.

Lipopolysaccharide structure patterns analysis

Examination of LPS structure pattern was done using slightly modified Marolda method of extraction (42) and SDS-PAGE. Overnight bacterial cultures in TSB medium (bioMerieux, France) were centrifuged and adjusted to OD_{600} = 2.0 in PBS buffer. Bacterial cells were destroyed by boiling in lysis buffer (2% SDS, 4% β-mercaptoethanol, Tris, pH 6.8) and digesting with proteinase K (60°C, 1h). Protein debris were eliminated by incubation (70°C, 15 min.) with equal volume of 90% phenol. LPS containing aqueous phase was recovered using ethyl ether to remove any residual phenol. Subsequently, the LPS samples were separated by Tricin SDS-PAGE method (14% polyacrylamide gel with 4M urea, 125 V). Finally, after separation, LPS samples were stained with silver according to Tsai & Frasch (43).

Biofilm production

The intensity of biofilm production was measured using crystal violet (CV) staining method in accordance with O'Toole and Kolter methodology (44) with slight modifications. Bacterial isolates were cultured (48h / 37°C) in TSB medium (bioMerieux, France) on 96-well peg-lid plates (Nunc, Denmark). After incubation, the biofilm formed on the surface of pegs was stained with 0.01% CV (15 min / 37°C), eluted with 96% ethanol and the OD_{590} was measured. Each sample was performed in at least eight replicates.

TLR stimulation profile in THP1-XBlue™ cell line, NF-kB/AP-1- Reporter Monocytes

The Toll-like receptors (TLRs) stimulation of monocytes, major forms of innate immune sensors, was assessed according to manufacturer protocol using THP1-XBlue™ cell line (InvivoGen, Toulouse France). THP1-XBlue™ cells derive from the human monocytic THP-1 cell line and express an NF-κB- and AP-1-inducible secreted embryonic alkaline phosphatase (SEAP) reporter gene. Upon TLR2, TLR1/2, TLR2/6, TLR4, TLR5 and TLR8 stimulation, THP1-XBlue™ cells activate transcription factors and subsequently the secretion of SEAP

which is easily detectable when using QUANTI-Blue™, a medium that turns purple/blue in the presence of SEAP.

Galleria mellonella larvae infection model

The virulence of PAO1 mutants resistant to PA5oct phage was tested *in vivo* in *G. mellonella* infection model, previously described by Cullen et al. (17). The wax moth larvae were sorted by size and weight and acclimated for one week at 15°C. The larvae were infected by the injection into the hindmost proleg, of 10 µl of bacterial suspension (10^3 cfu/ml) giving 10 cells per larvae. Further, the larvae were incubated at 37°C for 72h, and their viability was checked after 8, 18, 24, 48 and 72 hours post injection. The two types of control were made: in negative control larvae were injected with 10µl of sterile PBS buffer, while the positive control consisted of wild PAO1 strain infection. The graphical presentation of the survival curves was prepared using GraphPad Prism 6.0 (GraphPad Software Inc., La Jolla, USA). The log-rank Mantel-Cox test was used for statistical analysis (P-values < 0.05 were regarded as significant).

Pseudolysogeny/lysogeny detection

The presence of PA5oct genome within the cells of PAO1 resistant mutants was evaluated using a standard polymerase chain reaction (PCR). The DNA was isolated using PureLink Genomic DNA mini kit (Invitrogen, Thermo Scientific). On the basis of the full sequence of PA5oct genome, primers flanking a fragment of the structural gene (major head subunit precursor) were designed (F: 5'-GATACATACCCTACGTGTTCGTTATG-3' and R: 5'-GCACCGTTACCCAGCGAGTTAG). The PCR was carried out under the optimized conditions: initialization (95°C / 5 min), 30 cycles of denaturation (95°C / 30 s), annealing (56.4°C / 1 min) and elongation (72°C / 1 min 10 s) followed by final elongation (72°C / 10 min). The resulting 872 bp reaction product was visualized by standard agarose gel electrophoresis (1% agarose, 1X TBE buffer, 95 V/cm / 45 min.). The positive control was a purified PA5oct phage preparation and the negative control was a PAO1 strain. The episome state (pseudolysogeny) of PA5oct was confirmed by PFGE analysis according to previously described protocol (16).

Acknowledgements. This study was supported by research grant 2012/04/M/NZ6/00335 and 2015/18/M/NZ6/00413 of National Science Centre, Poland. RL is supported by a GOA grant entitled "Phage Biosystems" from the KU Leuven.

Bibliography

1. Wittebole X, De Roock S, Opal SM. 2014. A historical overview of bacteriophage therapy as an alternative to antibiotics for the treatment of bacterial pathogens. Virulence **5**:226–235. doi:10.4161/viru.25991.

2. Forti F, Roach DR, Cafora M, Pasini ME, Horner DS, Fiscarelli E V., Rossitto M, Cariani L, Briani F, Debarbieux L, Ghisotti D. 2018. Design of a broad-range bacteriophage cocktail that reduces *Pseudomonas aeruginosa* biofilms and treats acute infections in two animal models. Antimicrob Agents Chemother **62**:e02573-17. doi:10.1128/AAC.02573-17.

3. Galtier M, De Sordi L, Sivignon A, de Vallée A, Maura D, Neut C, Rahmouni O, Wannerberger K, Darfeuille-Michaud A, Desreumaux P, Barnich N, Debarbieux L. 2017. Bacteriophages targeting adherent invasive *Escherichia coli* strains as a promising new treatment for Crohn's disease. J Crohn's Colitis **11**:840–847. doi:10.1093/ecco-jcc/jjw224.

4. Roach DR, Leung CY, Henry M, Morello E, Singh D, Di Santo JP, Weitz JS, Debarbieux L. 2017. Synergy between the host immune system and bacteriophage is essential for successful phage therapy against an acute respiratory pathogen. Cell Host Microbe **22**:38–47.e4. doi:10.1016/j.chom.2017.06.018.

5. Pirnay J-P, Verbeken G, Ceyssens P-J, Huys I, De Vos D, Ameloot C, Fauconnier A. 2018. The Magistral phage. Viruses **10**:64. doi:10.3390/v10020064.

6. Hendrix RW. 2009. Jumbo bacteriophages. Curr Top Microbiol Immunol **328**:229–240. doi:10.1007/978-3-540-68618-7-7.

7. Yuan Y, Gao M. 2017. Jumbo bacteriophages: An overview. Front Microbiol **8**:doi:10.3389/fmicb.2017.00403.

8. Monson R, Foulds I, Foweraker J, Welch M, Salmond GPC. 2011. The *Pseudomonas aeruginosa* generalized transducing phage phiPA3 is a new member of the phiKZ-like group of "jumbo" phages, and infects model laboratory strains and clinical isolates from cystic fibrosis patients. Microbiology **157**:859–67. doi:10.1099/mic.0.044701-0.

9. Lecoutere E, Ceyssens PJ, Miroshnikov KA, Mesyanzhinov V V., Krylov VN, Noben JP, Robben J, Hertveldt K, Volckaert G, Lavigne R. 2009. Identification and comparative

analysis of the structural proteomes of φKZ and EL, two giant *Pseudomonas aeruginosa* bacteriophages. Proteomics **9**:3215–3219. doi:10.1002/pmic.200800727.

10. Mesyanzhinov V V, Robben J, Grymonprez B, Kostyuchenko VA, Bourkaltseva M V, Sykilinda NN, Krylov VN, Volckaert G. 2002. The genome of bacteriophage φKZ of *Pseudomonas aeruginosa*. J Mol Biol **317**:1–19. doi:10.1006/jmbi.2001.5396.

11. Fokine A, Battisti AJ, Bowman VD, Efimov A V., Kurochkina LP, Chipman PR, Mesyanzhinov V V., Rossmann MG. 2007. Cryo-EM Study of the *Pseudomonas* bacteriophage φKZ. Structure **15**:1099–1104. doi:10.1016/j.str.2007.07.008.

12. Ceyssens P-J, Minakhin L, Van den Bossche A, Yakunina M, Klimuk E, Blasdel B, De Smet J, Noben J-P, Blasi U, Severinov K, Lavigne R. 2014. Development of giant bacteriophage phiKZ is independent of the host transcription apparatus. J Virol **88**:10501–10510. doi:10.1128/JVI.01347-14.

13. Chaikeeratisak V, Nguyen K, Khanna K, Brilot AF, Erb ML, Coker JKC, Vavilina A, Newton GL, Buschauer R, Pogliano K, Villa E, Agard DA, Pogliano J. 2017. Assembly of a nucleus-like structure during viral replication in bacteria. Science **355**:194–197. doi:10.1126/science.aal2130.

14. Krylov VN, Dela Cruz DM, Hertveldt K, Ackermann H-W. 2007. "φKZ-like viruses", a proposed new genus of myovirus bacteriophages. Arch Virol **152**:1955–1959. doi:10.1007/s00705-007-1037-7.

15. Danis-Wlodarczyk K, Vandenheuvel D, Jang H Bin, Briers Y, Olszak T, Arabski M, Wasik S, Drabik M, Higgins G, Tyrrell J, Harvey BJ, Noben J-P, Lavigne R, Drulis-Kawa Z. 2016. A proposed integrated approach for the preclinical evaluation of phage therapy in *Pseudomonas* infections. Sci Rep **6**:28115. doi:10.1038/srep28115.

16. Drulis-Kawa Z, Olszak T, Danis K, Majkowska-Skrobek G, Ackermann H-W. 2014. A giant *Pseudomonas* phage from Poland. Arch Virol **159**:567–572. doi:10.1007/s00705-013-1844-y.

17. Cullen L, Weiser R, Olszak T, Maldonado R, Moreira A, Slachmuylders L, Brackman G, Paunova-Krasteva T, Zarnowiec P, Czerwonka G, Reilly J, Drevinek P, Kaca W, Melter O, De Soyza A, Perry A, Winstanley C, Stoitsova SR, Lavigne R, Mahenthiralingam E, Sa-Correia I, Coenye T, Drulis-Kawa Z, Augustyniak D, Valvano MA, McClean S. 2015. Phenotypic characterization of an international *Pseudomonas*

aeruginosa reference panel: strains of cystic fibrosis (CF) origin show less in vivo virulence than non-CF strains. Microbiology **161**:1961–1977. doi:10.1099/mic.0.000155.

18. Pirnay J-P, De Vos D, Cochez C, Bilocq F, Vanderkelen A, Zizi M, Ghysels B, Cornelis P. 2002. *Pseudomonas aeruginosa* displays an epidemic population structure. Environ Microbiol **4**:898–911. doi:10.1046/j.1462-2920.2002.00321.x.

19. Zabner J, Karp P, Seiler M, Phillips SL, Mitchell CJ, Saavedra M, Welsh M, Klingelhutz AJ. 2003. Development of cystic fibrosis and noncystic fibrosis airway cell lines. Am J Physiol Cell Mol Physiol **284**:L844–L854. doi:10.1152/ajplung.00355.2002.

20. Olszak T, Zarnowiec P, Kaca W, Danis-Wlodarczyk K, Augustyniak D, Drevinek P, de Soyza A, McClean S, Drulis-Kawa Z. 2015. *In vitro* and *in vivo* antibacterial activity of environmental bacteriophages against *Pseudomonas aeruginosa* strains from cystic fibrosis patients. Appl Microbiol Biotechnol **99**:6021–6033. doi:10.1007/s00253-015-6492-6.

21. Worlitzsch D, Tarran R, Ulrich M, Schwab U, Cekici A, Meyer KC, Birrer P, Bellon G, Berger J, Weiss T, Botzenhart K, Yankaskas JR, Randell S, Boucher RC, Döring G. 2002. Effects of reduced mucus oxygen concentration in airway *Pseudomonas infections* of cystic fibrosis patients. J Clin Invest **109**:317–325. doi:10.1172/JCI200213870.

22. Abedon ST. 2016. Bacteriophage exploitation of bacterial biofilms: phage preference for less mature targets? FEMS Microbiol Lett **363**:fnv246. doi:10.1093/femsle/fnv246.

23. Azeredo J, Sutherland I. 2008. The use of phages for the removal of infectious biofilms. Curr Pharm Biotechnol **9**:261–266. doi:10.2174/138920108785161604.

24. Pires DP, Oliveira H, Melo LDR, Sillankorva S, Azeredo J. 2016. Bacteriophage-encoded depolymerases: their diversity and biotechnological applications. Appl Microbiol Biotechnol **100**:2141–2151. doi:10.1007/s00253-015-7247-0.

25. De Soyza A, Hall AJ, Mahenthiralingam E, Drevinek P, Kaca W, Drulis-Kawa Z, Stoitsova SR, Toth V, Coenye T, Zlosnik JE a, Burns JL, Sá-Correia I, De Vos D, Pirnay J-P, J Kidd T, Reid D, Manos J, Klockgether J, Wiehlmann L, Tümmler B, McClean S, Winstanley C. 2013. Developing an international *Pseudomonas aeruginosa* reference panel. Microbiologyopen **2**:1010–1023. doi:10.1002/mbo3.141.

26. Lorè NI, Cigana C, De Fino I, Riva C, Juhas M, Schwager S, Eberl L, Bragonzi A. 2012. Cystic fibrosis-niche adaptation of *Pseudomonas aeruginosa* reduces virulence in multiple infection hosts. PLoS One **7**:e35648. doi:10.1371/journal.pone.0035648.

27. Bradbury RS, Reid DWEC, Inglis TJJ, Champion AC. 2011. Decreased virulence of cystic fibrosis *Pseudomonas aeruginosa* in *Dictyostelium discoideum*. Microbiol Immunol **55**:224–230. doi:10.1111/j.1348-0421.2011.00314.x.

28. Cigana C, Curcurù L, Leone MR, Ieranò T, Lorè NI, Bianconi I, Silipo A, Cozzolino F, Lanzetta R, Molinaro A, Bernardini ML, Bragonzi A. 2009. *Pseudomonas aeruginosa* exploits lipid A and muropeptides modification as a strategy to lower innate immunity during cystic fibrosis lung infection. PLoS One **4**:e8439. doi:10.1371/journal.pone.0008439.

29. Le S, Yao X, Lu S, Tan Y, Rao X, Li M, Jin X, Wang J, Zhao Y, Wu NC, Lux R, He X, Shi W, Hu F. 2014. Chromosomal DNA deletion confers phage resistance to *Pseudomonas aeruginosa*. Sci Rep **4**:4738. doi:10.1038/srep04738.

30. Shen M, Zhang H, Shen W, Zou Z, Lu S, Li G, He X, Agnello M, Shi W, Hu F, Le S. 2018. *Pseudomonas aeruginosa* MutL promotes large chromosomal deletions through non-homologous end joining to prevent bacteriophage predation. Nucleic Acids Res doi:10.1093/nar/gky160.

31. Argov T, Azulay G, Pasechnek A, Stadnyuk O, Ran-Sapir S, Borovok I, Sigal N, Herskovits AA. 2017. Temperate bacteriophages as regulators of host behavior. Curr Opin Microbiol **38**:81–87. doi:10.1016/j.mib.2017.05.002.

32. Latino L, Midoux C, Hauck Y, Vergnaud G, Pourcel C. 2016. Pseudolysogeny and sequential mutations build multiresistance to virulent bacteriophages in *Pseudomonas aeruginosa*. Microbiol (United Kingdom) **162**:748–763. doi:10.1099/mic.0.000263.

33. Krylov V, Shaburova O, Krylov S, Pleteneva E. 2012. A genetic approach to the development of new therapeutic phages to fight *Pseudomonas aeruginosa* in wound infections. Viruses **5**:15–53. doi:10.3390/v5010015.

34. Danis-Wlodarczyk K, Olszak T, Arabski M, Wasik S, Majkowska-Skrobek G, Augustyniak D, Gula G, Briers Y, Jang H Bin, Vandenheuvel D, Duda KA, Lavigne R, Drulis-Kawa Z. 2015. Characterization of the newly isolated lytic bacteriophages KTN6 and KT28 and their efficacy against *Pseudomonas aeruginosa* biofilm. PLoS One

10:e0127603. doi:10.1371/journal.pone.0127603.

35. Ceyssens P-J, Lavigne R, Mattheus W, Chibeu A, Hertveldt K, Mast J, Robben J, Volckaert G. 2006. Genomic analysis of *Pseudomonas aeruginosa* phages LKD16 and LKA1: establishment of the KMV subgroup within the T7 supergroup. J Bacteriol **188**:6924–6931. doi:10.1128/JB.00831-06.

36. Ceyssens P-J, Mesyanzhinov V, Sykilinda N, Briers Y, Roucourt B, Lavigne R, Robben J, Domashin A, Miroshnikov K, Volckaert G, Hertveldt K. 2008. The genome and structural proteome of YuA, a new *Pseudomonas aeruginosa* phage resembling M6. J Bacteriol **190**:1429–1435. doi:10.1128/JB.01441-07.

37. Adams MH. 1959. Enumeration of phage particles, p. 27–30. *In* Adams, MH (ed.), Bacteriophages. Interscience Publishers, New York.

38. Kutter E. 2009. Phage host range and efficiency of plating. Methods Mol Biol **501**:141–149. doi:10.1007/978-1-60327-164-6_14.

39. Turnbull L, Whitchurch CB. 2014. Motility assay: twitching motility, p. 73–86. *In* Filloux, A, Ramos, J-L (eds.), *Pseudomonas* Methods and Protocols. Humana Press Inc., New York.

40. Ha D-G, Kuchma SL, O'Toole GA. 2014. Plate-based assay for swimming motility in *Pseudomonas aeruginosa*, p. 59–66. *In* Filloux, A, Ramos, JL (eds.), *Pseudomonas* Methods and Protocols. Humana Press Inc., New York.

41. Ha D-G, Kuchma SL, O'Toole GA. 2014. Plate-based assay for swarming motility in *Pseudomonas aeruginosa*, p. 73–86. *In* Filloux, A, Ramos, JL (eds.), *Pseudomonas* Methods and Protocols. Humana Press Inc., New York.

42. Marolda CL, Welsh J, Dafoe L, Valvano MA. 1990. Genetic analysis of the O7-polysaccharide biosynthesis region from the *Escherichia coli* O7:K1 strain VW187. J Bacteriol **172**:3590–3599. .

43. Tsai CM, Frasch CE. 1982. A sensitive silver stain for detecting lipopolysaccharides in polyacrylamide gels. Anal Biochem **119**:115–119. doi:10.1016/0003-2697(82)90673-X.

44. O'Toole G a, Kolter R. 1998. Flagellar and twitching motility are necessary for *Pseudomonas aeruginosa* biofilm development. Mol Microbiol **30**:295–304. doi:10.1046/j.1365-2958.1998.01062.x.

Supplementary materials

Table S1. Main features of *Pseudomonas* phages used in the study.

Table S2. Phage activity comparison of fourteen different phages on *P. aeruginosa* strains from Military Hospital Neder-Over-Heembeek, Brussels, Belgium collection (18). Grey box –active, white box – no activity.

Figure S1. LPS profiles of PA5-phage-resistant clones analyzed in 14 % polyacrylamide/glycine-SDS gels.

Figure S2. The virulence of PA5-phage-resistant clones tested *in vivo* in *G. mellonella* infection model injected with 10 cells per larvae. The positive control consisted of PAO1 biofilm isolate infection. The log-rank Mantel-Cox test was used for statistical analysis (denoted *P*-values < 0.05).

Figure S3. THP-1 X-blue monocyte response to PA5-phage-resistant clones post-culture medium stimulation.

Figure S4. PCR analysis targeting the major head subunit precursor gene in selected PA5oct resistant clones. M-mass marker.

Figure S5. Pulse-field gel electrophoresis (PFGE) of selected PA5oct resistant clones DNA material. YCM- yeast chromosome marker.